The Journal of Clinical Endocrinology & Metabolism, 2021, Vol. 106, No. 4, e1868–e1879
doi:10.1210/clinem/dgaa654
Clinical Research Article

Clinical Research Article

Long-term Bone Loss and Deterioration of Microarchitecture After Gastric Bypass in African American and Latina Women

Alexandra Krez,[1] Sanchita Agarwal,[2] Mariana Bucovsky,[2] Donald J. McMahon,[1,2] Yizhong Hu,[3] Marc Bessler,[4] Beth Schrope,[4] Angela Carrelli,[2] Shannon Clare,[1] Xiang-Dong Edward Guo,[3] Shonni J. Silverberg,[2] and Emily M. Stein[1]

[1]Endocrinology and Metabolic Bone Disease Service, Hospital for Special Surgery, New York, New York; [2]Department of Medicine, Columbia University College of Physicians and Surgeons, New York, New York; [3]Bone Bioengineering Laboratory, Department of Biomedical Engineering, Columbia University, New York, New York; and [4]Department of Surgery, Columbia University College of Physicians and Surgeons, New York, NY

ORCiD number: 0000-0002-1463-5774 (E. M. Stein).

Received: 14 June 2020; Accepted: 14 September 2020; First Published Online: 16 September 2020; Corrected and Typeset: 24 October 2020.

Abstract

Context: The prevalence of obesity is burgeoning among African American and Latina women; however, few studies investigating the skeletal effects of bariatric surgery have focused on these groups.

Objective: To investigate long-term skeletal changes following Roux-en-Y gastric bypass (RYGB) in African American and Latina women.

Design: Four-year prospective cohort study.

Patients: African American and Latina women presenting for RYGB (n = 17, mean age 44, body mass index 44 kg/m^2) were followed annually for 4 years postoperatively.

Main Outcome Measures: Dual-energy x-ray absorptiometry (DXA) measured areal bone mineral density (aBMD) at the spine, hip, and forearm, and body composition. High-resolution peripheral quantitative computed tomography measured volumetric bone mineral density (vBMD) and microarchitecture. Individual trabecula segmentation-based morphological analysis assessed trabecular morphology and connectivity.

Results: Baseline DXA Z-Scores were normal. Weight decreased ~30% at Year 1, then stabilized. Parathyroid hormone (PTH) increased by 50% and 25-hydroxyvitamin D was stable. By Year 4, aBMD had declined at all sites, most substantially in the hip. There was significant, progressive loss of cortical and trabecular vBMD, deterioration of microarchitecture, and increased cortical porosity at both the radius and tibia over 4 years. There was loss of trabecular plates, loss of axially aligned trabeculae, and decreased trabecular connectivity. Whole bone stiffness and failure

ISSN Print 0021-972X ISSN Online 1945-7197
Printed in USA

load declined. Risk factors for bone loss included greater weight loss, rise in PTH, and older age.

Conclusions: African American and Latina women had substantial and progressive bone loss, deterioration of microarchitecture, and trabecular morphology following RYGB. Further studies are critical to understand the long-term skeletal consequences of bariatric surgery in this population.

Freeform/Key Words: bariatric surgery, bone loss, minority women, microarchitecture

The prevalence of obesity in the United States is burgeoning among racial and ethnic minorities. African American women have the highest rates of obesity compared with other groups; approximately 4 out of 5 are overweight or obese (1). Similarly, among Latina women in the United States, 79% are overweight or obese, as compared with 64% of non-Latina Caucasian women (2). While bariatric surgery has become an increasingly common and effective treatment for obesity (3–12), the majority of studies concerning the salutary and adverse effects of bariatric surgery have focused on Caucasian populations. Despite the high prevalence of obesity among African American and Latina women, less is known about the consequences of bariatric surgery in these patients.

Most studies have reported bone loss by dual-energy X-ray absorptiometry (DXA) in the first 1 to 2 years following bariatric surgery. Losses are most pronounced following Roux-en-Y gastric bypass (RYGB) procedures (13–17). Early declines in hip bone mass density (BMD) have been noted, ranging between 5% and 15% (13, 14, 17–26). Loss of volumetric bone mineral density (vBMD) and deterioration of peripheral bone microarchitecture have also been documented during the first 2 postoperative years (13, 17, 19, 27). There are limited data available regarding changes in skeletal structure beyond 2 years. Whether there may be ongoing long-term skeletal changes is of particular concern given recent reports of increased fracture risk following bariatric surgery, particularly RYGB (28–31).

The goal of this study was to investigate the long-term changes in bone microarchitecture following RYGB in a cohort of African American and Latina women using high-resolution peripheral quantitative computed tomography (HR-pQCT). Further, we sought to expand current knowledge by applying a novel technique, individual trabecula segmentation (ITS)-based morphological analysis to HR-pQCT to evaluate changes in trabecular morphology. We hypothesized that there would be a deterioration of microarchitecture, as well as a loss of trabecular plates and connectivity following RYGB.

Methods

We prospectively enrolled women with obesity who had planned RYGB surgery between January 2009 and June 2015 at the Columbia University Medical Center (CUMC) Obesity Surgery Center. Patients were recruited prior to surgery and monitored for 4 years afterward. RYGB procedures at CUMC included a 20-mL gastric pouch, a 150-cm Roux-limb, and a 75-cm biliopancreatic limb. Prior to preoperative study baseline, all patients met with a nutritionist. All preoperative and postoperative supplementation was done as part of clinical care by the surgical nutrition team. Patients were given the following clinical recommendations. Those who were between 19 and 50 years of age were prescribed calcium citrate 1500 mg daily in divided doses. Patients who were over the age of 50 were prescribed calcium citrate 1800 mg daily in divided doses. In addition, all patients were instructed to start a multivitamin. Patients found to have 25-hydroxyvitamin D (25OHD) levels below 20 ng/ml were started on 50 000 IU of vitamin D (ergocalciferol) 1 to 3 times per week preoperatively, with higher doses given to more severely deficient patients. Patients with levels above 20 ng/ml preoperatively received daily vitamin D in their calcium supplements and multivitamin. Calcium and vitamin D supplementation was continued postoperatively for all patients. All patients were prescribed 50 000 IU of vitamin D per week, and adjustments were made as needed by the clinical nutrition team. Subjects were asked about supplement use at each visit but compliance was not formally assessed. Patients with a baseline body weight that exceeded our DXA machine limit of 300 pounds were excluded. Other exclusion criteria included prior bariatric surgery and conditions and medications that could cause secondary osteoporosis. Of 179 women screened, 38 met eligibility criteria and signed consent. Common reasons for exclusion included patient preference, weight over 300 pounds, other type of bariatric procedure, and prior bariatric surgery. Those who completed 2-year follow-up were given the option to extend participation for 2 additional years. Seventeen women participated in the 4-year study.

The CUMC Institutional Review Board approved this study. All subjects provided written informed consent. Visits were performed at baseline and annually after surgery. Dietary calcium and vitamin D were assessed by a questionnaire, using the Dietary Calcium Rapid Assessment

method (32). Serum was obtained for calciotropic hormones and bone turnover markers. DXA was used to measure areal bone mineral density (aBMD) and body composition. HR-pQCT was used to measure vBMD, as well as cortical and trabecular microstructure at the distal radius and tibia. Changes to preoperative comorbidities were assessed by self-report and confirmed by chart review. Postmenopause was defined as 1 year after cessation of menses. Participants were asked about regular menses and any changes to menses as well as surgical menopause, last menstrual period, cycle length, and duration.

Biochemistries

Serum calcium, albumin, and creatinine were measured using automated techniques. 25-hydroxyvitamin D2 and D3 (25OHD2, 25OHD3) were measured by Ultra-performance Liquid Chromatography combined with tandem mass spectrometry (UPLC-MS/MS), using a 1290 UPLC and a 6410 Tandem Mass Spectrometer (Agilent, Santa Clara, California). Interassay coefficient of variation (CV) was 2.9% for 25OHD2 and 5.4% for 25OHD3. Intact parathyroid hormone (PTH) was measured by Immunoradiometric Assay (CV 6.8%; Scantibodies Laboratories, Santee, California). Serum C-telopeptide (CTX) was measured by ELISA (CV <10%; Immunodiagnostics Systems, Scottsdale, Arizona). Serum osteocalcin (OC) was measured by ELISA (CV 2.7%; Immunodiagnostic Systems). Bone specific alkaline phosphatase (BSAP) was measured by ELISA (CV 7.6%; Quidel Corporation, San Diego, California). Sclerostin was measured by ELISA (CV 9.4%; TECO Medical Group, Sissach, Switzerland). Blood was drawn fasting, prior to 10:00 AM. Serum was archived at -80°C and analyzed in 1 batch after all subjects had completed their study visits.

aBMD and body composition

Areal BMD was measured by DXA (QDR-4500; Hologic Inc., Waltham, Massachusetts) at the lumbar spine (L1-L4; LS), total hip (TH), femoral neck (FN), and 1/3 radius. Z-scores compared subjects and controls with age-matched populations of the same sex and race/ethnicity, as provided by the manufacturer. Total fat mass, truncal fat, and lean mass were measured by DXA. The short-term in vivo precision is 0.90% for the spine, 1.36% for the FN, and 0.70% for the radius.

HR-pQCT and finite element analysis of the distal radius and tibia

HR-pQCT (XtremeCT, Scanco Medical AG, Brüttisellen, Switzerland) was performed on the nondominant forearm and ipsilateral distal tibia, as described (33). The region of interest was defined by the manual placement of a reference line at the endplate of the distal radius or tibia using a 2-demensional scout scan. The first slice was obtained at 9.5 mm and 22.5 mm proximal to the reference line at the radius and tibia, respectively. A 3-dimensional (3D) image of approximately 9 mm in the axial direction was acquired, generating a stack of 110 parallel CT slices, using an effective energy of 40 keV, image matrix size of 1024 x 1024, and a nominal voxel size of 82 µm. Attenuation data were converted to equivalent hydroxyapatite (HA) densities. Phantom provided by the manufacturer was scanned daily for quality control. The analytic methods have been described, validated, and applied in recent clinical studies (34–36). HR-pQCT data was used to calculate whole bone stiffness and failure load, surrogate measures of the bone's resistance to force, as we have previously described (34). During the follow-up period, a second-generation of the HR-pQCT (Xtreme CT-II; XCT2) was acquired by CUMC. Five follow-up scans were acquired using this machine. Correction factor was developed, with an extensive cross calibration study at CUMC (37), and was used to convert all XCT2 data to make them comparable to the first-generation scanner.

Cortical porosity

To evaluate the cortical bone structure, a validated autosegmentation method (38) was applied to separate the cortical and trabecular compartments and measure cortical porosity (%). Cortical porosity was calculated as the percentage of void space in the cortex. This method has been validated for accuracy (39) and reproducibility (40), and is distributed by Scanco Medical.

ITS-based morphological analyses of HR-pQCT images

The trabecular bone compartment of each HR-pQCT image was manually extracted and separated from the cortex (36). All trabecular bone images were then subjected to ITS-based morphological analyses. A complete volumetric decomposition technique was applied to segment the trabecular network into individual plates and rods (41). Briefly, digital topological analysis (DTA)-based skeletonization (42) was applied first to transform a trabecular bone image into a representation composed of surfaces and curves skeleton while preserving the topology (ie, connectivity, tunnels, and cavities) (43, 44), as well as the rod and plate morphology of the trabecular microarchitecture. Then, digital topological classification was applied in which each skeletal voxel was uniquely

classified as either a surface or a curve type (45). Using an iterative reconstruction method, each voxel of the original image was classified as belonging to either an individual plate or rod. Based on the 3D evaluations of each individual trabecular plate and rod, bone volume and plate and rod number were evaluated by plate and rod bone volume fraction (pBV/TV and rBV/TV) and tissue fraction (pBV/BV and rBV/BV), as well as plate and rod number densities (pTb.N and rTb.N, 1/mm). Intactness of the trabecular network was characterized by plate-plate, plate-rod, and rod-rod junction density (P-P, P-R, and R-R Junc.D, 1/mm^3), calculated as the total junctions between trabecular plates and rods normalized by the bulk volume. The orientation of the trabecular bone network was characterized by axial bone volume fraction (aBV/TV), defined as axially aligned bone volume divided by the bulk volume. Detailed methods describing the complete volumetric decomposition technique and ITS-based measurements can be found in our prior publications (41, 46).

Statistical analysis

Descriptive data are presented as mean ± standard deviation (SD) for continuous measures and count (% of total) for categorical variables. A linear mixed model with a fixed effect for year postsurgery, coded as an integer, and first order autoregressive (AR1) covariance structure was used to evaluate the 4-year within-subject change in the biochemical and structural parameters. A secondary analysis of temporal trends in pre- versus postmenopausal women included menopausal status and menopausal status-by-time interaction as fixed effects in the linear model, as described above. Comparisons between baseline and follow-up time points are presented as the model estimated mean ± standard error of the mean (SEM) of the between-time difference with *P*-values from calculations of simultaneous confidence limits (SAS Proc MIXED). Fisher's exact test was used to estimate the change in categorical risk factors by year postsurgery, and Spearman's correlation was used to assess bivariate associations between change or percent change in risk factors with bone outcomes. No adjustments for multiple comparisons or the imput of missing data were applied. A formal sample size calculation was not performed; rather, all subjects who met eligibility criteria and were interested were consecutively enrolled.

Results

Seventeen women (mean age 43 ± 10 years) were followed prospectively before and for 4 years following RYGB. Mean baseline body mass index was 44 + 5 kg/m^2 and percent of body fat was 48 ± 5%. All subjects were Latina (71%) or African American (29%). Latina subjects were predominantly from the Caribbean. Nine subjects were premenopausal (53%) and 7 subjects were postmenopausal (41%). Many participants did not have regular menses at baseline, as is common in this population, but did not report menopausal symptoms or changes. One participant who was considered perimenopausal reported that her menses became irregular during Year 2 of study follow-up and had no further menses during Year 3 of study follow-up. Comorbidities related to obesity were common (47% of the subjects had diabetes mellitus, 76% had hypertension, 35% had hyperlipidemia, 47% had obstructive sleep apnea, and 53% had osteoarthritis). At study baseline, mean 25OHD levels were sufficient (44 ± 27 ng/ml), reflecting supplementation by the clinical nutritionist, prior to study enrollment. Serum calcium, PTH, creatinine, and albumin were within the normal range (Table 1).

Changes in weight and body composition

Substantial weight loss occurred during the first postoperative year (29 ± 3%, $P < 0.001$), and weight remained stable during the subsequent 3 years. Changes in body composition were also most pronounced over the first year. Total body fat declined by 17 ± 3% ($P < 0.001$) and trunk fat declined by 21 ± 3% ($P < 0.001$). Lean mass increased by 16 ± 3% ($P < 0.001$). There was no further change in total body fat, trunk fat, and lean mass between Year 1 and Year 4.

Table 1. Baseline clinical characteristics of study subjects

Characteristics	Baseline Mean ± Standard Deviation (SD), n (%)
Age	43 ± 10
Race/ethnicity	
African American (non-Latina)	5 (29%)
Latina	12 (71%)
Menopause status	
Premenopausal	9 (53%)
Perimenopausal	1 (6%)
Postmenopausal	7 (41%)
Body composition	
Weight (kg)	11 ± 13
Body mass index (kg/m^2)	44 ± 5
Lean mass (kg)	52 ± 5
Trunk fat (kg)	47 ± 6
Fat mass (kg)	48 ± 5
Calcium intake (mg/d)	860 ± 172
Vitamin D intake (IU/d)	9423 ± 2515[a]

[a]The majority of patients were taking 50 000 IU per week, as instructed by the clinical nutritionist.

Changes in comorbidities

Four years following RYGB, comorbidities had resolved or improved in the majority of patients. Among women with diabetes, the condition resolved in 38% of women and improved in the remaining 63%. Hypertension and hyperlipidemia resolved in approximately half of the women (46% and 50%, respectively) and improved in the remainder. Obstructive sleep apnea resolved in 13% and improved in 63%. Osteoarthritis resolved in 22% and improved in 33%. One woman sustained a fragility fracture of the tibia, which occurred in Year 4.

Changes in calciotropic hormones and bone turnover

Changes in biochemistries that occurred following RYGB are detailed in Table 2. There was no significant change in calcium or vitamin D intake from diet or supplements throughout the study. Serum-corrected calcium and creatinine remained stable throughout the study duration. Levels of 25OHD were similarly constant. In contrast, PTH rose incrementally after surgery, with a peak increase of 58 ± 19% ($P < 0.01$) at Year 4. Bone turnover markers increased most profoundly during Year 1. Bone resorption, measured by CTX, increased by 214 ± 59% ($P < 0.001$) 1 year after surgery. CTX remained elevated through Year 3, and then began to decrease, trending toward baseline by Year 4. Bone formation, measured by BSAP and OC, increased by 20 ± 8% ($P < 0.05$) and 153 ± 34% ($P < 0.001$) 1 year after surgery, respectively. While BSAP remained elevated throughout the 4-year study duration, OC mirrored CTX and decreased toward baseline between Years 3 and 4.

Changes in aBMD

Baseline Z-scores were above normal at all sites (LS Z-score: 1.2 ± 1.7, TH: 1.5 ± 1.7, FN: 1.5 ± 1.9, 1/3 radius: 1.3 ± 1.7). The changes in aBMD that occurred following RYGB are detailed in Fig. 1. During the first year following surgery, substantial bone loss occurred at the hip sites, both TH (-7.5 ± 1.4%, $P < 0.001$) and FN (-6.07 ± 1.7%, $P < 0.001$). Over the next 3 years, aBMD progressively declined at both hip sites, by 5.4 ± 1.8% at the TH ($P < 0.005$) and 6.0 ± 2.1% at the FN ($P < 0.01$). While there were no significant changes in aBMD at the spine during the first year, bone loss at the LS became apparent during Year 2 and continued over the following 2 years. By year 4, LS aBMD had decreased by 6.8 ± 1.3% ($P < 0.001$). Bone loss at the 1/3 radius fluctuated in the first 3 years, but had decreased significantly from baseline by Year 4 (-3.3 ± 1.5%, $P < 0.05$). Although values decreased over the 4 years, mean Z-Scores remained within the normal range at all sites.

Changes in vBMD and bone microarchitecture

HR-pQCT was used to investigate the 4-year progression of changes in vBMD and microarchitecture. The majority of changes that were observed during the first year were small and not significant. However, significant loss of vBMD and deterioration of microarchitecture became apparent after the first year and progressed over the subsequent 3 years. Pronounced changes in both cortical and trabecular bone occurred at the radius and tibia. Total density substantially declined at both sites over the 4 years (radius: -11%; $P < 0.001$, and tibia: -10%; $P < 0.001$). By Year 4, there were marked declines in cortical thickness (radius: -6%; $P < 0.001$, and tibia: -8%; $P < 0.001$), cortical area (radius: -6%; $P < 0.001$, and tibia: -10%; $P < 0.001$), and cortical density (radius: -3%; $P < 0.001$, and tibia: -7%; $P < 0.001$; Fig. 2). Cortical porosity increased progressively over the 4 years (radius: +51%; $P < 0.001$, and tibia: +55%; $P < 0.001$). Trabecular density decreased

Table 2. Longitudinal changes in calciotropic hormones and bone turnover markers (mean ± standard error [SE])

Calciotropic Indices	Baseline	Year 1	Year 2	Year 3	Year 4
Calcium (8.6–10.2mg/dL)	9.6 ± 0.1	9.5 ± 0.1	9.5 ± 0.1	9.5 ± 0.2	9.6 ± 0.1
PTH (14–66 pg/mL)	39 ± 5	43 ± 6	52 ± 6[b]	48 ± 8	59 ± 7[b]
25OHD (30–80 ng/mL)	44 ± 8	46 ± 6	40 ± 5	40 ± 7	43 ± 6
CTX (0.112–0.738 ng/mL)	0.25 ± 0.04	0.64 ± 0.10[a]	0.67 ± 0.09[a]	0.69 ± 0.13[b]	0.43 ± 0.11
BSAP (11.6–42.7 U/L)	29.5 ± 2.1	35.5 ± 2.4[b]	31.1 ± 2.3	32.8 ± 3.3	35.8 ± 2.7[b]
Osteocalcin (8.4–33.9 ng/mL)	14.3 ± 2.0	31.9 ± 2.0[a]	29.9 ± 1.9[a]	29.4 ± 2.0[a]	18.0 ± 3.0
Sclerostin (0.17–1.21 ng/mL)	0.58 ± 0.06	0.59 ± 0.03	0.63 ± 0.03	0.55 ± 0.04	0.56 ± 0.03

Abbreviations: 25OHD, 25-hydroxy vitamin D; BSAP, bone specific alkaline phosphatase; CTX, C-telopeptide; PTH, parathyroid hormone.
[a] P-Value ≤0.001 for comparison to baseline;
[b]P-Value ≤0.05 for comparison to baseline.

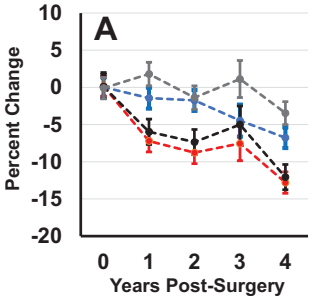

Figure 1. Longitudinal changes in areal bone mineral density (aBMD) by dual-energy x-ray absorptiometry (DXA) over 4 years following Roux-en-Y gastric bypass (RYGB). The red line represents total hip, the blue line lumbar spine, the black line femoral neck, and the grey line 1/3 radius.

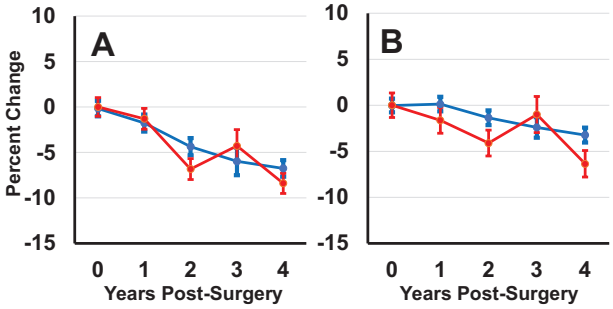

Figure 2. Longitudinal changes in cortical volumetric bone mineral density (BMD) and thickness at the radius (**A**) and tibia (**B**). The red line represents cortical thickness and the blue line represents cortical density.

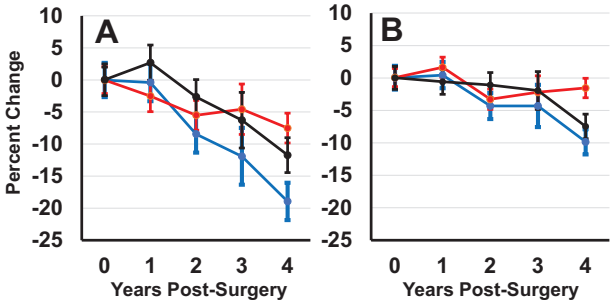

Figure 3. Longitudinal changes in trabecular volumetric bone mineral density (BMD) over 4 years following Roux-en-Y gastric bypass (RYGB) at the radius (**A**) and tibia (**B**). The red line represents trabecular number, the blue line represents trabecular density, and the black line represents trabecular thickness.

(radius: -19%; $P < 0.001$, and tibia: -10%; $P < 0.001$) and trabecular microarchitecture deteriorated, with declines in trabecular number (radius: -8%; $P < 0.01$, and tibia: -2%; $P = 0.31$) and thickness (radius: -12%; $P < 0.001$, and tibia: -7%; $P < 0.001$; Fig. 3). Raw data is presented in Table 3.

Trabecular microstructure, orientation, and connectivity

Changes in trabecular microstructure, orientation, and connectivity manifested after Year 1 and progressed throughout the next 3 years. At both the radius and tibia, there were substantial losses in the overall volume of trabecular plates (radius: -12%; $P < 0.05$, and tibia: -9%; $P < 0.01$) and number of plates (radius: -5%; $P < 0.01$, and tibia: -3%; $P < 0.01$). The number of axially aligned trabeculae declined (radius: -12%; $P < 0.01$, and tibia: -7%; $P < 0.05$). There was a loss of connectivity of the network between trabecular plates (radius: -13%; $P < 0.01$, and tibia: -6%; $P < 0.01$) and between plates and rods (radius: -12%; $P < 0.001$, and tibia: -4%; $P = 0.16$; Fig. 4).

Biomechanical properties of bone

There were substantial, progressive declines in whole bone stiffness and failure load at both sites over the 4-year study duration. By year 4, whole bone stiffness declined by 12 ± 3% ($P < 0.001$) at the radius and 10 ± 2% ($P < 0.001$) at the tibia. Failure load declined by 13 ± 2% ($P < 0.001$) at the radius and 9 ± 2% ($P < 0.01$) at the tibia.

Predictors of skeletal changes

Greater weight loss, rise in PTH, older age, and postmenopausal status were found to be the most important risk factors for bone loss following RYGB. Patients who lost the most weight also had the most bone loss. Weight loss following RYGB was associated with bone loss at axial sites as measured by DXA (LS [r = 0.36, $P < 0.05$], TH [r = 0.70, $P < 0.001$], FN [r = 0.43, $P < 0.01$]). By HR-pQCT, those who lost the most weight had more bone loss at both the tibia (total density [r = 0.41, $P < 0.01$], cortical density [r = 0.54, $P < 0.001$], and cortical thickness [r = 0.43, $P < 0.01$]), and radius (total density [r = 0.38, $P < 0.05$] and cortical thickness [r = 0.41, $P < 0.01$]).

Patients who had a greater rise in PTH had more declines in areal bone density measured by DXA at the total hip (r = -0.33, $P < 0.05$). The relationship between rise in PTH and bone loss at the 1/3 radius did not reach statistical significance (r = -0.25, $P = 0.11$). Rise in PTH correlated with cortical thinning at the tibia (r = -0.36, $P < 0.05$) and radius (r = -0.38, $P < 0.05$) and loss of vBMD (tibia: total density [r = -0.32, $P < 0.05$], and trabecular density [r = -0.34, $P < 0.05$]; radius: total density [r = -0.46, $P < 0.01$]). Further, an increase in PTH was associated with a decrease in stiffness (r = -0.41, $P < 0.01$) at the radius only.

Older patients had more bone loss measured by DXA at the spine and FN (LS aBMD, r = -0.53, $P < 0.001$; FN

Table 3. Raw data fromHR-pQCT and ITS-based morphologic analysis at baseline and Year 4 (mean ± SD)

	RADIUS		TIBIA	
	Baseline	Year 4	Baseline	Year 4
HR-pQCT				
Ct density (mg/HA^3)	929 ± 53	900 ± 83	897 ± 45	836 ± 74
Ct_thickness (mm)	0.939 ± 0.163	0.872 ± 0210	1.26 ± 0.23	1.13 ± 0.27
Ct_porosity (%)	0.012 ± 0.009	0.017 ± 0.013	0.038 ± 0.017	0.058 ± 0.027
Total density (mg/HA^3)	374 ± 59	333 ± 67	318 ± 55	283 ± 44
Tb density (mg/HA^3)	159 ± 39	128 ± 46	175 ± 32	154 ± 37
Tb Number (1/mm)	1.99 ± 0.31	1.86 ± 0.31	1.94 ± 0.25	1.91 ± 0.21
Tb thickness (mm)	0.067 ± 0.012	0.057 ± 0.013	0.075 ± 0.011	0.068 ± 0.012
Tb separation (mm)	0.449 ± 0.084	0.497 ± 0.107	0.450 ± 0.077	0.465 ± 0.064
Heterogeneity (mm)	0.183 ± 0.045	0.181 ± 0.091	0.204 ± 0.045	0.180 ± 0.091
Whole bone stiffness (N/mm)	51 094 ± 11 947	45 147 ± 12 631	140 163 ± 27 794	126 756 ± 27 499
ITS				
Total bone volume fraction	0.279 ± 0.052	0.245 ± 0.060	0.301 ± 0.038	0.282 ± 0.040
Plate bone volume fraction	0.096 ± 0.047	0.073 ± 0.040	0.148 ± 0.041	0.129 ± 0.043
Plate Tb number (1/mm)	1.40 ± 0.19	1.30 ± 0.19	1.55 ± 0.11	1.50 ± 0.13
Axial bone volume fraction	0.099 ± 0.035	0.081 ± 0.032	0.134 ± 0.029	0.121 ± 0.030
Plate-plate junction density (1/mm^3)	1.94 ± 0.69	1.56 ± 0.66	2.37 ± 0.45	2.18 ± 0.49
Plate-rod junction density (1/mm^3)	4.05 ± 1.20	3.45 ± 1.15	4.20 ± 0.75	3.99 ± 0.61

Abbreviations: HR-pQCT, high resolution peripheral quantitative computed tomography; ITS, individual trabecula segmentation; SD, standard deviation; Ct, cortical; Tb, trabecular.

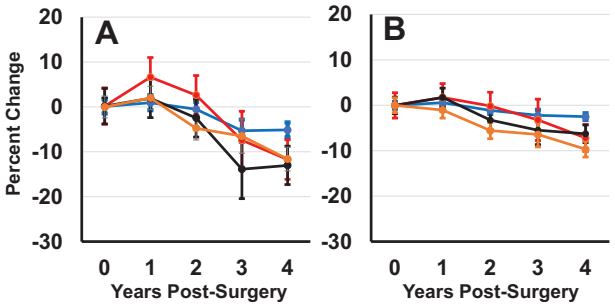

Figure 4. Longitudinal changes in trabecular morphology, orientation, and connectivity over 4 years following Roux-en-Y gastric bypass (RYGB) at the radius (**A**) and tibia (**B**). The red line represents axial bone volume fraction, the blue line represents plate trabecular number, the black line represents plate-plate junction density, and the orange line represents whole bone stiffness.

aBMD, r = -0.53, $P < 0.001$). Older patients also had greater losses by HR-pQCT. Age was more closely related to cortical bone loss at both the radius and tibia (radius: total density [r = -0.43, $P < 0.01$] and cortical thickness [r = -0.55, $P < 0.001$]; tibia: total density [r = -0.38, $P < 0.05$], cortical density [r = -0.50, $P < 0.001$], and cortical thickness [r = -0.39, $P < 0.05$]). Menopause status was also investigated as a risk factor for postoperative bone loss. For these analyses, the postmenopausal group included the subject that became postmenopausal during follow-up. Postmenopausal women had greater declines in aBMD at all sites, in particular at the LS, over the 4 years compared with premenopausal women. By HR-pQCT, postmenopausal women had greater declines in total density, cortical density, and cortical thickness (Table 4). There was no difference in bone loss by DXA, HR-pQCT, or FEA, according to baseline diabetes status.

Table 4. Difference in Year 4 bone loss after RYGB according to menopausal status

Variable	RADIUS			TIBIA		
	% Difference	SE	*P*	% Difference	SE	*P*
Ct density	-4.45	1.71	0.01	-6.62	1.41	0.00
Ct_thickness	-10.91	2.47	0.00	-9.51	1.48	0.00
Ct_porosity	38.82	22.25	0.09	55.81	14.67	0.00
Total density	-8.03	3.10	0.01	-5.68	2.40	0.02
Tb density	4.06	6.07	0.51	4.23	4.02	0.30
Tb Number	-4.96	5.01	0.33	-4.19	3.08	0.18
Tb thickness	9.20	5.30	0.09	7.18	3.71	0.06
Tb separation	6.76	7.42	0.37	2.44	3.66	0.51
Heterogeneity	50.83	13.19	0.00	42.53	9.67	0.00
Whole bone stiffness	-2.13	5.89	0.72	-3.97	3.75	0.30

Data presented are the percent difference in rates of bone loss over the 4-year study period between pre- and postmenopausal women. Premenopausal women are used as the reference.
Abbreviations: RYGB, Roux-en-Y gastric bypass; SE, standard error; Ct, cortical; Tb, trabecular.

Discussion

While bone loss following bariatric surgery has been demonstrated in several cohorts, this is the first study, to our knowledge, that has focused on long-term skeletal changes in African American and Latina women. Our findings suggest that although these women may enter surgery with normal BMD, they experience pronounced bone loss that extends for at least 4 years afterward. While weight loss was confined to the first postoperative year, substantial, progressive deterioration of density and microarchitecture continued 4 years following RYGB. We extend the findings of prior studies of microarchitecture by using ITS to investigate changes in trabecular morphology, orientation, and connectivity. We found that there were detrimental changes in trabecular morphology, loss of plates, orientation, and connectivity that manifested after the first year and continued for up to 4 years.

Given the prevalence of obesity among African American and Latina women, it is critical to understand the long-term beneficial and harmful effects of bariatric surgery, the most effective treatment for sustained weight loss, in this population. Several studies have documented racial and ethnic differences in bone mass (47-49). Our group (50), and others (51), have shown that bone microarchitecture and trabecular microstructure differ according to race and ethnicity. The baseline skeletal differences between women of different ethnicities demonstrated in these prior reports raised the question of whether the skeletal response to bariatric surgery would differ. Our study found that African American and Latina women had pronounced changes to bone mass, microarchitecture, and strength, similar to those reported in Caucasian populations. However, there were also some important differences noted.

The majority of studies investigating bone loss after bariatric surgery have focused on the first 1 or 2 postoperative years. The 4-year duration of our study enabled us to relate the bone loss and microarchitectural deterioration to the timing and progression of postoperative weight loss. While we observed profound weight loss during the first year, changes in microarchitecture were small. In contrast, despite stabilization of weight, microarchitectural deterioration became more apparent and progressive over the next 3 years. While some prior studies have reported early changes in microarchitecture, others have not (13–15, 19). Our findings suggest that this discrepancy may be due to the fact that the initial changes are too small to detect in some cohorts. The later occurring declines in microarchitecture we observed did not plateau by year 4, raising concern that losses may extend beyond our study duration. Very few prospective studies have assessed microarchitecture changes beyond 2 years following RYGB (17, 52). Significant cortical and trabecular deterioration have been observed between the second and fifth postoperative years (17) and the second and seventh postoperative years (52). We observed similar declines in cortical density, area, and thickness at the radius to Lindeman and colleagues, and further observed losses in cortical area, trabecular thickness, and trabecular separation at the tibia between the first and fourth postoperative years. As that study enrolled predominantly Caucasian patients, differences in the racial composition of our cohorts may have contributed to discrepancies in our findings.

While ITS has been used to further investigate the skeletal morphology of other populations (53–57), this is the first prospective application of ITS in patients undergoing bariatric surgery. This 3D model independent technique provides additional information regarding trabecular characteristics and connectivity that directly relate to biomechanical properties of bone (41, 46, 58, 59). While we did not detect any substantial changes in trabecular morphology during the first postoperative year, by the fourth year, women had fewer trabecular plates, fewer axially aligned trabeculae and less connectivity between trabeculae. These changes are concerning because all of these features are directly related to decreased strength (41, 46, 58, 59). Trabecular deterioration was observed at both sites, but was most pronounced at the radius. This finding parallels our observations of standard HR-pQCT measures in this cohort and may reflect the preservation of trabecular microstructure at the tibia, a weight-bearing skeletal site. These longitudinal data support and extend the findings of a recent cross-sectional study that reported fewer trabecular plates and fewer axially aligned trabeculae in patients 10 years after RYGB compared with body mass index–matched controls (60).

Our study confirmed the uniform finding of decreased hip aBMD by DXA 1 year following bariatric surgery (13, 14, 17–26). Declines at the TH and FN persisted for 4 years and, similar to the microarchitectural changes, did not appear to plateau. The magnitude of these losses at Year 4 in our study corresponds to observations in other long-term prospective cohorts (17, 25, 52). Reports of short-term changes at the spine have been inconsistent, with some studies reporting declines and others showing no change. We did not observe changes at the spine over the first year, similar to prior observations by our group (13, 23). However, bone loss at the spine manifested by Year 2 and continued throughout Year 4. To our knowledge, this is the first prospective study to measure bone density at the 1/3 radius 4 years following RYGB. Interestingly, while measurements at the radius fluctuated, they were significantly below baseline by the fourth postoperative year. This is not unexpected, given the increase in PTH levels observed over the course of the study.

Several mechanisms have been proposed to explain the bone loss observed following RYGB, including skeletal

unloading, abnormalities in calciotropic hormones, and changes in gut hormones. The unloading hypothesis is supported by the initial preferential bone loss at the weight-bearing hip as well as the strong correlation between the extent of weight loss and the amount of bone loss in this and other studies (13, 23, 61–64). However, it is notable that weight remained stable between Year 1 and Year 4, the period corresponding to the greatest declines in bone density, deterioration of cortical and trabecular bone microarchitecture, and changes in trabecular morphology. Similar to our findings, other studies have reported ongoing bone loss after weight loss plateaued (17, 19). While it is conceivable that early substantial weight loss induces changes that extend far beyond the time when weight loss stabilizes, these findings suggest that other factors likely contribute to the ongoing bone loss as well. In our cohort, advanced age correlated with greater declines in bone density. Our findings, however, cannot be attributed to age alone, as the magnitude of bone loss that we observed far exceeded expected age related losses (65, 66). Our results also suggest that postmenopausal women are at higher risk for bone loss following RYGB. This result is similar to findings by Schafer et al, who documented that postmenopausal women had more dramatic increases in bone resorption and bone deterioration at peripheral sites 1 year following RYGB (15). The bone loss at the LS and TH in postmenopausal women in our study is far greater than the annual changes reported in studies of the general postmenopausal population (65, 66). Further, we found that the most pronounced declines were at the hip sites and not at the spine, as would result from menopausal estrogen loss. Overall, our results suggest that aging and estrogen deficiency may compound the detrimental skeletal effects of bariatric surgery. These findings suggest that clinicians should consider postmenopausal women undergoing bariatric surgery to be at particular risk for deleterious skeletal outcomes.

We found that PTH levels rose despite the fact that patients in our cohort were supplemented with calcium and vitamin D preoperatively and throughout the postoperative period. A greater rise in PTH after surgery was a risk factor for cortical thinning and decreased bone stiffness. This finding suggests that despite normal serum levels of calcium and vitamin D, more subtle perturbations in absorption of these nutrients may occur. This observation is consistent with radiolabeled studies demonstrating calcium malabsorption despite supplementation (67, 68). The continued rise in PTH that we observed may have been related to a relatively inadequate calcium intake as well as reduced compliance with calcium supplements over time. The mean reported supplement intake for our patients was below the amount recommended by the clinical nutritionists. Further, although we did not formally assess compliance, other authors have shown that compliance with supplements after RYGB is poor, particularly beyond the first postoperative year (69). The rate of increase in markers of bone resorption and formation was the greatest in the first year following RYGB. While CTX remained elevated until Year 3, other studies have reported increases in CTX at Years 5 (17) and 7 (52) when compared with baseline. Comparable to our observations with OC, procollagen type I *N*-terminal propeptide (P1NP), another marker of bone formation, has been reported to increase short term, but trends toward baseline several years following bariatric surgery (17, 52).

Prior work by our group (13) and others has found that patients lose lean mass following RYGB (70, 71). Further, a correlation between bone loss and loss of lean body mass has been reported (27). In contrast to those findings, lean bone mass increased after RYGB among the women in our cohort. It is conceivable that this difference is due to differential effects of surgery on lean mass in African American and Latina women. Physical activity has been shown to lessen the loss of lean mass after surgery (21). We did not measure physical activity, so we cannot determine whether increased activity levels contributed to our findings. While loss of lean mass has been hypothesized to contribute to bone loss after surgery, the increase in lean mass that we observed did not appear to mitigate the effects of bone loss in our cohort. The data suggest that further studies in larger cohorts investigating the relationship between changes in lean mass and bone loss after bariatric surgery in minority women are needed. Additionally, these data speak against the hypothesis that loss of lean mass is an important driver of bone loss in those undergoing bariatric surgery.

Recent studies have suggested that fracture risk may be increased in patients following bariatric surgery. Although there are some conflicting reports (72), the risk appears to be most heightened after RYGB (28, 73) and other malabsorptive procedures (74). Fracture rates appear to increase several years after surgery (28, 31). Our findings suggest that prolonged deterioration of microarchitecture and trabecular morphology may be an underlying mechanism for the increase in skeletal fragility among these individuals. They suggest that long-term monitoring of bone health is critical following RYGB.

Our study has unique strengths and important limitations. To our knowledge, this is the first long-term study of skeletal changes after bariatric surgery in African American and Latina women, groups with extremely high rates of obesity (1, 2). We applied the novel technique of ITS to obtain information on prospective changes to trabecular morphology, orientation, and connectivity, which has not been previously reported. A major limitation of our study is the small sample size. While this is a common

limitation of prospective studies in this field, a greater number of subjects would have enabled us to further investigate the relationships and interactions between risk factors for bone loss, including differences among the Latina and African American women. We were unable to investigate risk factors for fractures in this cohort. We did not assess compliance to calcium and vitamin D supplements and so we could not determine whether decreased use of supplements contributed to some of the observed changes in biochemistries. We did not collect data on physical activity, which may have played a role in the observed changes at the weight-bearing hip and tibia. While obesity and changes in adiposity cause artifacts in DXA measurements (75–77), our use of HR-pQCT enabled us to obtain measurements less affected by surrounding adipose tissue.

In conclusion, African American and Latina women had substantial declines in bone density and deterioration of microarchitecture and trabecular morphology that persisted for 4 years following RYGB. While the initial bone loss at the hip corresponded to the period of maximum weight loss, changes in both cortical and trabecular bone continued long after the cessation of weight loss. These findings may provide a mechanism for the increased fractures seen several years after RYGB. Given the burgeoning rates of obesity among African American and Latina women, larger, long-term studies are critical to further understand the relationship between postoperative skeletal changes and fracture risk in this population.

Acknowledgments

Financial Support: This work was supported by K24 DK074457 and The Thomas L. Kempner and Katheryn C. Patterson Foundation.

Additional Information

Correspondence and Reprint Requests: Emily M. Stein, MD, MS, Director of Research, Metabolic Bone Service, Hospital for Special Surgery, Associate Professor of Medicine, Weill Cornell Medical College, 535 East 70th Street, New York, NY 10021, USA. E-mail: steine@hss.edu.

Disclosure Summary: M.B. is the founder of Endobetes, a startup focused on developing an endoscopic device for weight loss and diabetes. The other authors have no conflicts of interest.

Data Availability: Some or all datasets generated during and/or analyzed during the current study are not publicly available but are available from the corresponding author on reasonable request.

References

1. Obesity and African Americans. *U.S. Department of Health and Human Services Office of Minority Health*. https://minorityhealth.hhs.gov/omh/browse.aspx?lvl=4&lvlid=25
2. Obesity and Hispanic Americans. *U.S. Department of Health and Human Services Office of Minority Health*. https://minorityhealth.hhs.gov/omh/browse.aspx?lvl=4&lvlid=70
3. Mechanick JI, Youdim A, Jones DB, et al.; American Association of Clinical Endocrinologists; Obesity Society; American Society for Metabolic & Bariatric Surgery. Clinical practice guidelines for the perioperative nutritional, metabolic, and nonsurgical support of the bariatric surgery patient–2013 update: cosponsored by American Association of Clinical Endocrinologists, The Obesity Society, and American Society for Metabolic & Bariatric Surgery. *Obesity (Silver Spring)*. 2013;**21**(Suppl 1):S1–27.
4. Buchwald H, Estok R, Fahrbach K, et al. Weight and type 2 diabetes after bariatric surgery: systematic review and meta-analysis. *Am J Med*. 2009;**122**(3):248–256.e5.
5. Angrisani L, Santonicola A, Iovino P, et al. Bariatric surgery and endoluminal procedures: IFSO Worldwide Survey 2014. *Obes Surg*. 2017;**27**(9):2279–2289.
6. Maciejewski ML, Arterburn DE, Van Scoyoc L, et al. Bariatric surgery and long-term durability of weight loss. *JAMA Surg*. 2016;**151**(11):1046–1055.
7. Schauer PR, Kashyap SR, Wolski K, et al. Bariatric surgery versus intensive medical therapy in obese patients with diabetes. *N Engl J Med*. 2012;**366**(17):1567–1576.
8. Mingrone G, Panunzi S, De Gaetano A, et al. Bariatric surgery versus conventional medical therapy for type 2 diabetes. *N Engl J Med*. 2012;**366**(17):1577–1585.
9. Chang SH, Stoll CR, Song J, Varela JE, Eagon CJ, Colditz GA. The effectiveness and risks of bariatric surgery: an updated systematic review and meta-analysis, 2003-2012. *JAMA Surg*. 2014;**149**(3):275–287.
10. Sjöström L, Peltonen M, Jacobson P, et al. Bariatric surgery and long-term cardiovascular events. *Jama*. 2012;**307**(1):56–65.
11. Adams TD, Gress RE, Smith SC, et al. Long-term mortality after gastric bypass surgery. *N Engl J Med*. 2007;**357**(8):753–761.
12. Sjöström L, Narbro K, Sjöström CD, et al.; Swedish Obese Subjects Study. Effects of bariatric surgery on mortality in Swedish obese subjects. *N Engl J Med*. 2007;**357**(8):741–752.
13. Stein EM, Carrelli A, Young P, et al. Bariatric surgery results in cortical bone loss. *J Clin Endocrinol Metab*. 2013;**98**(2):541–549.
14. Yu EW, Bouxsein ML, Putman MS, et al. Two-year changes in bone density after Roux-en-Y gastric bypass surgery. *J Clin Endocrinol Metab*. 2015;**100**(4):1452–1459.
15. Schafer AL, Kazakia GJ, Vittinghoff E, et al. Effects of gastric bypass surgery on bone mass and microarchitecture occur early and particularly impact postmenopausal women. *J Bone Miner Res*. 2018;**33**(6):975–986.
16. Goode LR, Brolin RE, Chowdhury HA, Shapses SA. Bone and gastric bypass surgery: effects of dietary calcium and vitamin D. *Obes Res*. 2004;**12**(1):40–47.
17. Lindeman KG, Greenblatt LB, Rourke C, Bouxsein ML, Finkelstein JS, Yu EW. Longitudinal 5-year evaluation of bone density and microarchitecture after Roux-en-Y gastric bypass surgery. *J Clin Endocrinol Metab*. 2018;**103**(11):4104–4112.
18. Bredella MA, Greenblatt LB, Eajazi A, Torriani M, Yu EW. Effects of Roux-en-Y gastric bypass and sleeve gastrectomy on bone mineral density and marrow adipose tissue. *Bone*. 2017;**95**:85–90.
19. Shanbhogue VV, Støving RK, Frederiksen KH, et al. Bone structural changes after gastric bypass surgery evaluated by

HR-pQCT: a two-year longitudinal study. *Eur J Endocrinol*. 2017;**176**(6):685–693.
20. Liu C, Wu D, Zhang JF, et al. Changes in bone metabolism in morbidly obese patients after bariatric surgery: a meta-analysis. *Obes Surg*. 2016;**26**(1):91–97.
21. Muschitz C, Kocijan R, Haschka J, et al. The impact of vitamin D, calcium, protein supplementation, and physical exercise on bone metabolism after bariatric surgery: the BABS study. *J Bone Miner Res*. 2016;**31**(3):672–682.
22. Nielson CM, Srikanth P, Orwoll ES. Obesity and fracture in men and women: an epidemiologic perspective. *J Bone Miner Res*. 2012;**27**(1):1–10.
23. Fleischer J, Stein EM, Bessler M, et al. The decline in hip bone density after gastric bypass surgery is associated with extent of weight loss. *J Clin Endocrinol Metab*. 2008;**93**(10):3735–3740.
24. Coates PS, Fernstrom JD, Fernstrom MH, Schauer PR, Greenspan SL. Gastric bypass surgery for morbid obesity leads to an increase in bone turnover and a decrease in bone mass. *J Clin Endocrinol Metab*. 2004;**89**(3):1061–1065.
25. Vilarrasa N, San José P, García I, et al. Evaluation of bone mineral density loss in morbidly obese women after gastric bypass: 3-year follow-up. *Obes Surg*. 2011;**21**(4):465–472.
26. Vilarrasa N, Gómez JM, Elio I, et al. Evaluation of bone disease in morbidly obese women after gastric bypass and risk factors implicated in bone loss. *Obes Surg*. 2009;**19**(7):860–866.
27. Schafer AL, Li X, Schwartz AV, et al. Changes in vertebral bone marrow fat and bone mass after gastric bypass surgery: A pilot study. *Bone*. 2015;**74**:140–145.
28. Yu EW, Lee MP, Landon JE, Lindeman KG, Kim SC. Fracture risk after bariatric surgery: Roux-en-Y gastric bypass versus adjustable gastric banding. *J Bone Miner Res*. 2017;**32**(6):1229–1236.
29. Fashandi AZ, Mehaffey JH, Hawkins RB, Schirmer B, Hallowell PT. Bariatric surgery increases risk of bone fracture. *Surg Endosc*. 2018;**32**(6):2650–2655.
30. Nakamura KM, Haglind EG, Clowes JA, et al. Fracture risk following bariatric surgery: a population-based study. *Osteoporos Int*. 2014;**25**(1):151–158.
31. Lu CW, Chang YK, Chang HH, et al. Fracture risk after bariatric surgery: a 12-year nationwide cohort study. *Medicine (Baltimore)*. 2015;**94**(48):1–7.
32. Hertzler AA, Frary RB. A dietary calcium rapid assessment method (RAM). *Top Clin Nutr*. 1994;**9**(3):76–85.
33. Stein EM, Liu XS, Nickolas TL, et al. Abnormal microarchitecture and reduced stiffness at the radius and tibia in postmenopausal women with fractures. *J Bone Miner Res*. 2010;**25**(12):2572–2581.
34. Laib A, Rüegsegger P. Calibration of trabecular bone structure measurements of in vivo three-dimensional peripheral quantitative computed tomography with 28-microm-resolution microcomputed tomography. *Bone*. 1999;**24**(1):35–39.
35. MacNeil JA, Boyd SK. Accuracy of high-resolution peripheral quantitative computed tomography for measurement of bone quality. *Med Eng Phys*. 2007;**29**(10):1096–1105.
36. Liu XS, Zhang XH, Sekhon KK, et al. High-resolution peripheral quantitative computed tomography can assess microstructural and mechanical properties of human distal tibial bone. *J Bone Miner Res*. 2010;**25**(4):746–756.
37. Agarwal S, Rosete F, Zhang C, et al. In vivo assessment of bone structure and estimated bone strength by first- and second-generation HR-pQCT. *Osteoporos Int*. 2016;**27**(10):2955–2966.
38. Buie HR, Campbell GM, Klinck RJ, MacNeil JA, Boyd SK. Automatic segmentation of cortical and trabecular compartments based on a dual threshold technique for in vivo micro-CT bone analysis. *Bone*. 2007;**41**(4):505–515.
39. Nishiyama KK, Macdonald HM, Buie HR, Hanley DA, Boyd SK. Postmenopausal women with osteopenia have higher cortical porosity and thinner cortices at the distal radius and tibia than women with normal aBMD: an in vivo HR-pQCT study. *J Bone Miner Res*. 2010;**25**(4):882–890.
40. Burghardt AJ, Buie HR, Laib A, Majumdar S, Boyd SK. Reproducibility of direct quantitative measures of cortical bone microarchitecture of the distal radius and tibia by HR-pQCT. *Bone*. 2010;**47**(3):519–528.
41. Liu XS, Sajda P, Saha PK, et al. Complete volumetric decomposition of individual trabecular plates and rods and its morphological correlations with anisotropic elastic moduli in human trabecular bone. *J Bone Miner Res*. 2008;**23**(2):223–235.
42. Saha PK, Chaudhuri BB, Majumder DD. A new shape preserving parallel thinning algorithm for 3D digital images. *Pattern Recogn*. 1997;**30**(12):1939–1955.
43. Saha PK, Chaudhuri BB. Detection of 3-D simple points for topology preserving. *IEEE Trans Pattern Anal Mach Intell*. 1994;**16**(10):1028–1032.
44. Saha PK, Chaudhuri BB, Chanda B, Majumder DD. Topology preservation in 3D digital space. *Pattern Recogn*. 1994;**27**:295–300.
45. Saha PK, Chaudhuri BB. 3D digital topology under binary transformation with applications. *Comput Vis Image Underst*. 1996;**63**(3):418–429.
46. Liu XS, Sajda P, Saha PK, Wehrli FW, Guo XE. Quantification of the roles of trabecular microarchitecture and trabecular type in determining the elastic modulus of human trabecular bone. *J Bone Miner Res*. 2006;**21**(10):1608–1617.
47. Hochberg MC. Racial differences in bone strength. *Trans Am Clin Climatol Assoc*. 2007;**118**:305–315.
48. Looker AC, Melton LJ 3rd, Harris TB, Borrud LG, Shepherd JA. Prevalence and trends in low femur bone density among older US adults: NHANES 2005-2006 compared with NHANES III. *J Bone Miner Res*. 2010;**25**(1):64–71.
49. Nelson DA, Beck TJ, Wu G, et al. Ethnic differences in femur geometry in the women's health initiative observational study. *Osteoporos Int*. 2011;**22**(5):1377–1388.
50. Zhou B, Wang J, Stein EM, et al. Bone density, microarchitecture and stiffness in Caucasian and Caribbean Hispanic postmenopausal American women. *Bone Res*. 2014;**2**:1–9.
51. Putman MS, Yu EW, Lee H, et al. Differences in skeletal microarchitecture and strength in African-American and white women. *J Bone Miner Res*. 2013;**28**(10):2177–2185.
52. Hansen S, Jørgensen NR, Hermann AP, Støving RK. Continuous decline in bone mineral density and deterioration of bone microarchitecture 7 years after Roux-en-Y gastric bypass surgery. *Eur J Endocrinol*. 2020;**182**(3):303–311.
53. Walker MD, Liu XS, Zhou B, et al. Premenopausal and postmenopausal differences in bone microstructure and

mechanical competence in Chinese-American and white women. *J Bone Miner Res*. 2013;**28**(6):1308–1318.
54. Liu XS, Walker MD, McMahon DJ, et al. Better skeletal microstructure confers greater mechanical advantages in Chinese-American women versus white women. *J Bone Miner Res*. 2011;**26**(8):1783–1792.
55. Liu XS, Cohen A, Shane E, et al. Individual trabeculae segmentation (ITS)-based morphological analysis of high-resolution peripheral quantitative computed tomography images detects abnormal trabecular plate and rod microarchitecture in premenopausal women with idiopathic osteoporosis. *J Bone Miner Res*. 2010;**25**(7):1496–1505.
56. Liu XS, Stein EM, Zhou B, et al. Individual trabecula segmentation (ITS)-based morphological analyses and microfinite element analysis of HR-pQCT images discriminate postmenopausal fragility fractures independent of DXA measurements. *J Bone Miner Res*. 2012;**27**(2):263–272.
57. Sutter S, Nishiyama KK, Kepley A, et al. Abnormalities in cortical bone, trabecular plates, and stiffness in postmenopausal women treated with glucocorticoids. *J Clin Endocrinol Metab*. 2014;**99**(11):4231–4240.
58. Liu XS, Bevill G, Keaveny TM, Sajda P, Guo XE. Micromechanical analyses of vertebral trabecular bone based on individual trabeculae segmentation of plates and rods. *J Biomech*. 2009;**42**(3):249–256.
59. Fields AJ, Lee GL, Liu XS, Jekir MG, Guo XE, Keaveny TM. Influence of vertical trabeculae on the compressive strength of the human vertebra. *J Bone Miner Res*. 2011;**26**(2):263–269.
60. Lindeman KG, Rushin CC, Cheney MC, Bouxsein ML, Hutter MM, Yu EW. Bone density and trabecular morphology at least 10 years after gastric bypass and gastric banding. *J Bone Miner Res*. 2020;**00**(00):1sf.
61. Giusti V, Gasteyger C, Suter M, Heraief E, Gaillard RC, Burckhardt P. Gastric banding induces negative bone remodelling in the absence of secondary hyperparathyroidism: potential role of serum C telopeptides for follow-up. *Int J Obes (Lond)*. 2005;**29**(12):1429–1435.
62. Salamone LM, Cauley JA, Black DM, et al. Effect of a lifestyle intervention on bone mineral density in premenopausal women: a randomized trial. *Am J Clin Nutr*. 1999;**70**(1):97–103.
63. Riedt CS, Cifuentes M, Stahl T, Chowdhury HA, Schlussel Y, Shapses SA. Overweight postmenopausal women lose bone with moderate weight reduction and 1 g/day calcium intake. *J Bone Miner Res*. 2005;**20**(3):455–463.
64. Schwartz AV, Johnson KC, Kahn SE, et al.; Look AHEAD Research Group. Effect of 1 year of an intentional weight loss intervention on bone mineral density in type 2 diabetes: results from the Look AHEAD randomized trial. *J Bone Miner Res*. 2012;**27**(3):619–627.
65. Finkelstein JS, Brockwell SE, Mehta V, et al. Bone mineral density changes during the menopause transition in a multiethnic cohort of women. *J Clin Endocrinol Metab*. 2008;**93**(3):861–868.
66. Neer RM; SWAN Investigators. Bone loss across the menopausal transition. *Ann N Y Acad Sci*. 2010;**1192**:66–71.
67. Riedt CS, Brolin RE, Sherrell RM, Field MP, Shapses SA. True fractional calcium absorption is decreased after Roux-en-Y gastric bypass surgery. *Obesity (Silver Spring)*. 2006;**14**(11):1940–1948.
68. Schafer AL, Weaver CM, Black DM, et al. Intestinal calcium absorption decreases dramatically after gastric bypass surgery despite optimization of vitamin D status. *J Bone Miner Res*. 2015;**30**(8):1377–1385.
69. Agaba EA, Smith K, Normatov I, et al. Post-gastric bypass vitamin therapy: how compliant are your patients and who is doing the monitoring? *J Obes Bariatrics*. 2015;**2**(2):1–5.
70. Alba DL, Wu L, Cawthon PM, et al. Changes in lean mass, absolute and relative muscle strength, and physical performance after gastric bypass surgery. *J Clin Endocrinol Metab*. 2019;**104**(3):711–720.
71. Maghrabi AH, Wolski K, Abood B, et al. Two-year outcomes on bone density and fracture incidence in patients with T2DM randomized to bariatric surgery versus intensive medical therapy. *Obesity (Silver Spring)*. 2015;**23**(12):2344–2348.
72. Lalmohamed A, de Vries F, Bazelier MT, et al. Risk of fracture after bariatric surgery in the United Kingdom: population based, retrospective cohort study. *Bmj*. 2012;**345**:1–11.
73. Zhang Q, Chen Y, Li J, et al. A meta-analysis of the effects of bariatric surgery on fracture risk. *Obes Rev*. 2018;**19**(5):728–736.
74. Rousseau C, Jean S, Gamache P, et al. Change in fracture risk and fracture pattern after bariatric surgery: nested case-control study. *BMJ*. 2016;**354**:1–11.
75. Binkley N, Krueger D, Vallarta-Ast N. An overlying fat panniculus affects femur bone mass measurement. *J Clin Densitom*. 2003;**6**(3):199–204.
76. Yu EW, Thomas BJ, Brown JK, Finkelstein JS. Simulated increases in body fat and errors in bone mineral density measurements by DXA and QCT. *J Bone Miner Res*. 2012;**27**(1):119–124.
77. Knapp KM, Welsman JR, Hopkins SJ, Fogelman I, Blake GM. Obesity increases precision errors in dual-energy X-ray absorptiometry measurements. *J Clin Densitom*. 2012;**15**(3):315–319.